Mathematical Modelling of Engineering Problems
Vol. 9, No. 2, April, 2022, pp. 411-417
Journal homepage: http://iieta.org/journals/mmep

Influence of Strut Geometry on the Size Effect of FRP Reinforced Simply Supported Deep Beams: A Theoretical Analysis

Othman Hameed Zinkaah*, Hussein Kareem Sultan, Ali Al-Rifaie, Zainab Alridha

Department of Civil Engineering, Al-Muthanna University, Samawah 66001, Iraq

Corresponding Author Email: othman.h.zinkaah@mu.edu.iq

https://doi.org/10.18280/mmep.090215

Received: 29 August 2021
Accepted: 21 January 2022

Keywords:
deep beams, fibre reinforced polymer bars, size effect, strut and tie method, bearing plates

ABSTRACT

The reduction in the shear strength accompanied to the increasing in the section depth is characterised as size effect, assuming that all parameters are kept constant. Such behaviour is controlled by many factors. The geometry of the element formed between the load and support points is one of those factors that need to be highlighted. Owing to that, this study aims to assess the impact of the strut geometry on the size effect from the strut and tie method (STM) point of view. As the strut geometry is represented by bearing plates and concrete cover, the current study has focused on those two parameters. Accordingly, two groups of specimens have been examined analytically using STM of the American, European and Canadian codes. In each group, three depths were used of 500, 100, and 1500 mm. The only differences between those two groups are dimensions of bearing plates (loading and supporting) and concrete cover. In the first group, the dimensions of bearing plates and concrete cover have been kept constant with 250 mm and 60 mm, respectively regardless of the section depth. In the second group, those two parameters have been proportioned with the section height to be 15% and 8% of section height, respectively. Furthermore, an experimental database of 25 deep beams reinforced with polymer bars has been compiled from the literature to evaluate the ability of the STM to consider the size effect. The results showed that STM does not consider the size effect. Additionally, the collected data confirmed that the STM of American and European codes overestimated the shear capacity, while the STM of Canadian code gave a conservative prediction, highlighting the need of suitable models for shear strength prediction of FRP reinforced deep elements.

1. INTRODUCTION

Size effect is the decreasing in the shear strength accompanied by the increasing in the member size. Since the specimen size in the laboratory is usually smaller than the actual size of the structural members, studying the effect of increasing member size attracted the attention of researchers and practitioners. Size effect can be indicated by normalizing the shear stress at failure ($V/b_w d$). Concrete compressive strength can be used to normalize shear load if the strengths of concrete are varied, thus the shear load can be ($V/f_c' \, b_w d$), where V is the shear capacity, b_w is the width of the beam, d is the effective depth and f_c' is the concrete compressive strength. Considerable investigations are available for FRP reinforced deep beams; however limited discussions are introduced for size effect analysis for such elements [1-3].

Due to the brittle behaviour of the members reinforced with FRP bars, it is believed that size effect in deep elements reinforced with FRP bars is more pronounced than those reinforced with steel bars. Nehdi et al. [4], Abed et al. [5] and Kim et al. [6] have assessed the influence of the member size on the shear strength of FRP reinforced simple deep beams, however more explanations are required to clarify the effect of member size on the shear strength. Andermatt and Lubell [7] have given a clear conclusion that as long as the width of bearing plates to the beam height ratio (l_p/h) is kept constant, size effect can be mitigated, especially when shear span/depth (a/d) ratio increases, as shown in Figure 1. The same conclusion has been confirmed but for deep beams reinforced with steel bars [8, 9]. According to the existing STM of American, European, and Canadian codes, the size effect can be eliminated as long as compressive strength, shear span to overall depth ratio, longitudinal reinforcement, and the width of bearing plates-to-the beam height ratio are kept constant. However, a contradicted results were reported in some of previous investigations [10, 11].

This paper seeks to study the size effect of FRP reinforced deep members from STM's point of view. The effect of the inclined compressive strut geometry on the size effect has been discussed using analytical simulation for two groups of samples. Furthermore, to evaluate the performance of existing standards for size effect prediction, results of 25 samples have been compiled from the literature to compare the measured results with the predicted ones.

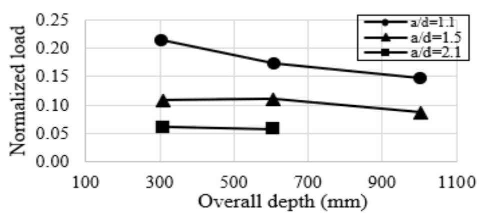

Figure 1. Size effect results [7]

2. REASONS OF THE SIZE EFFECT

Weibull [12] attributed the reduction in the shear strength while increasing the section depth to the difference in the strength of materials. Weibull has assumed that the concrete member consists of links of chain so that increase the section depth of the concrete leads to an increase in the number of links, resulting in higher probability of failure. However, some investigations proved that after the occurrence of the diagonal cracks, the reserve capacity (cracking load/ ultimate load) is found to be high enough to carry the external load, especially in the deep elements, and as a result the failure of one link in a concrete member does not lead to a rapid collapse of concrete [13].

Taylor [14] confirmed that aggregate interlock reduces with an increase in the section depth as long as keeping all parameters constant that in turn decreases the shear strength of the member. However, Walraven and Lehwalter [11] have found that aggregate interlock has no impact on the size effect; to assess whether the aggregate interlock is the reason of size effect, they have used light weight aggregate to study the impact of section size, because the interlocking effect of light weight aggregate can be neglected. The cracks in light weight concrete intersect the aggregate particles, while in normal weight aggregate cracks are running around the aggregate particles as shown in Figure 2. The results showed that a considerable size effect has occurred when lightweight aggregate was used, indicating that Taylor's theorem is inadequate to explain the size effect as the aggregate interlock has no effect on the size effect [11].

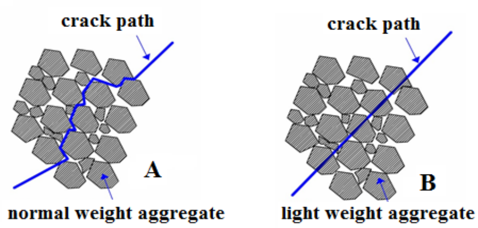

Figure 2. Crack paths for (A) normal weight concrete (B) Light weight concrete

Good number of researchers has explained the size effects in terms of fracture mechanics [10, 11, 15-19]. They argued that the released stored energy, brittleness, and crack propagation increase with the increase in the section depth.

Bazant and Planas [20] have argued that a same fracture energy is required to form a unit length of crack in both small and large beams. Since the area of the cross hatched strip (shown in Figure 3) in large beams is larger than that of small beams, the energy released in large beams will be higher. Such high released energy in large size beams leads to more crack propagations.

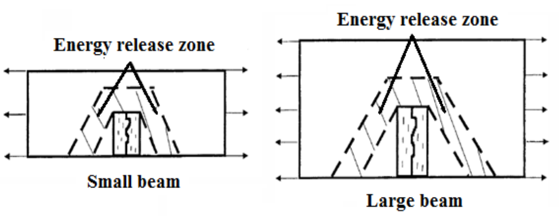

Figure 3. Sketch to explain size effect

The other reason making the small beams carry larger stress is that the crack widths in small size beams are lower than those of larger size ones. According to Wolinski et al. [21], tensile stresses can be transmitted up to about 0.20 mm of crack width as shown in Figure 4. Thus, higher tensile stresses can be transmitted in small size beams, resulting in higher shear stresses. It is worth mentioning that for elements reinforced with FRP bars, CSA S6 [22] has restricted the maximum crack widths for interior and exterior exposure elements by 0.35 mm and 0.25 mm, respectively.

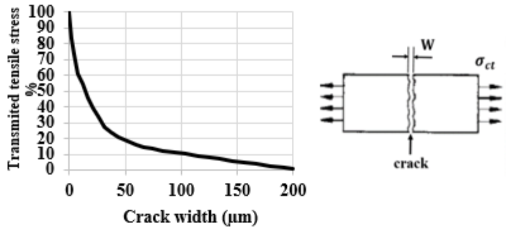

Figure 4. Transmitted stresses vs crack width curves of concrete [20]

Kotsovos and Pavlovic [23] have attributed the size effect to the unintended out of plane actions resulted from the beam the slim cross-section and non-symmetrical cracks which are experimentally unavoidable due to the heterogeneous nature of concrete. The out of plane actions occurs due to small unintended eccentricities of the applied load and hence leads to small stresses. The small stresses, in turn, lead to a significant reduction of the load carrying capacity of the large size concrete members. It is found that the presence of stirrups can minimize the effect of non-symmetrical cracks and hence size effects can be eliminated. However, the stresses induced from the out of plane action was found to be very small and can be ignored [24, 25].

Tan et al. [13] highlighted that the term of shear strength definition, V/bd, is unsuitable to reflect the size effect of concrete members, and this term is more appropriate to study the size effect of steel beams. With increasing the applied load, the depth of cracked tension zone increases which leads to inconstant concrete effective depth, d. Thus, the uncracked region of shear stress distribution will reduce, however the V/bd term takes the value of d constant. Regardless the value V/bd, no other term has been introduced to study the size effect, furthermore the crack baths are distributed along the concrete member regardless the section depth which means that the same conditions are applied for all member when the V/bd term is used.

To the author's view, most of mentioned factors are reasons for size effect, but they are different in their impact. Released energy can be considered as the main reason followed by aggregate interlock, while the out of plain action is active only in beams with large depths and have a high ratio of overall depth to beam width (h/b). Moreover, the brittle behaviour of the structural members makes size effect more pronounced.

3. STRUT AND TIE METHOD OF AMERICAN, EUROPEAN AND CANADIAN CODES

Right now, the strut and tie method (STM) of the American and European codes does not consider the effect of polymer (FRP) bars on the behavior of deep beams. However, the STM of the Canadian standards of elements reinforced with FRP bars (S806-2012) utilized the same term that was recommended by CSA A23.3-04 for deep elements reinforced with steel bars [26]. Strut and tie method is based on the lower bound theory which means that the failure load calculated from the equilibrium equations is less than or equal to the true collapse load [26, 27]. The STM analyses concrete members as a truss which transfers the loads between loading and supporting points. Struts and ties carry the compression and tension stresses, respectively as shown in Figure 5.

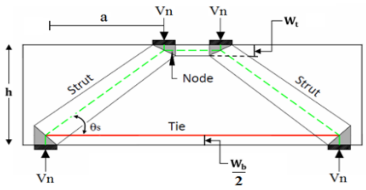

Figure 5. Typical STM for elements under two applied loads

CSA A23.3-84 [28] was the first design code to adopt the STM as a standard design technique of concrete members with disturbed regions, while American code (ACI 318-02) [29] has adopted the STM in its Appendix A in 2002. Struts and ties are connected at nodes and their forces can be determined using the equilibrium equations. STM is a suitable method for deep elements of nonlinear strain distribution. Eq. (1) is the general term used to calculate the predicted shear strengths of the assessed STMs [30-32], taking the strut efficiency factor (βs) according to Table 1.

$$V_n = \beta_s f_c' A_{strut} \sin\theta_s \tag{1}$$

where, $f_c^{`}$ is the compressive strength of concrete, A_{strut} is the area of concrete strut that will described further in section 4, and θ_s is the angle between the strut and tie. The stress limits in the nodal zones of American, European and Canadian codes are taken according to Table 2.

Table 1. Strut efficiency factor according to ACI 318-14, Euro EN-2004 and CSA-S806-12 codes

Code	Strut efficiency factor (βs)	
ACI 318-14 [32]	Bottle-shaped strut achieving reinforcement required by ACI 318-14	0.64
	Bottle-shaped strut does not achieve the reinforcement required by ACI 318-14	0.51
EN 2004 [30]	(For strut with transverse tension) $0.6(1-\frac{f_{ck}}{250})$, f_{cK} is the characteristic compressive strength and equal to f_c'	
CSA-S806-12 [31]	$\frac{1}{0.8+170\varepsilon_1} \le 0.85$, $\varepsilon_1 = [\varepsilon_f + (\varepsilon_f + 0.002)cot^2\theta_s]$, ε_1 is the principal tensile strain and ε_f is the tensile strain in the FRP bar	

Table 2. Stresses limits in the nodal zones according to ACI 318-14, EN 2-2004 and CSA-S806-12 codes

Code	Node efficiency factor (βn)		
	Nodes bounded by compression (CCC)	Nodes anchoring one tie (CCT)	Nodes with more than one tie (CTT and TTT Nodes)
ACI 318-14 [32]	$0.85f_c'$	$0.68f_c'$	$0.51f_c'$
EN 2004 [30]	$0.6(1-\frac{f_{c^`}}{250})f_c'$	$0.51(1-\frac{f_{c^`}}{250})f_c'$	$0.51(1-\frac{f_{c^`}}{250})f_c'$
CSA-S806-12 [31]	$0.85f_c'$	$0.75f_c'$	$0.65f_c'$

4. STRUT GEOMETRY AND SIZE EFFECT ACCORDING TO THE STM

Some investigations have argued that the geometry of concrete strut is one of the main factors that governs the size effect [8, 9, 33, 34]. This part of study aims to assess such effect in terms of STM. According to the STM, the cross-sectional area in the bottom and the top ends of the diagonal concrete strut can be determined from Eq. (2) and Eq. (3), respectively, as shown in Figure 6a and 6b.

$$A_{(strut)b} = b_w(W_b \cos\theta_s + L_b \sin\theta_s) \tag{2}$$

$$A_{(strut)t} = b_w(W_t \cos\theta_s + L_t \sin\theta_s) \tag{3}$$

where $A_{(strut)t}$ and $A_{(strut)b}$ are the areas of the top and bottom ends of concrete strut, respectively, b_w is the web width, W_t and W_b are the depth of the top and bottom nodal zones, respectively, L_t and L_b are the widths of the loading and supporting bearing plates, respectively (Figure 6). The angle between inclined compressive strut and tie is calculated as follows:

$$tan\theta_s = \frac{h - \frac{W_t}{2} - \frac{W_b}{2}}{a} \tag{4}$$

where a is the distance between the load and support points. American code [32] and Canadian highway bridge design code [22] have specified how to calculate the width of the concrete strut, while European code did not address any method to calculate such width. However, all codes have taken STM from the same reference [27].

The area of concrete strut depends on: i) the angle (θ) between the inclined concrete strut and reinforcement tie, ii) width of the bearing plates (l_b), and iii) the concrete cover (C_b) as the depth of top and bottom nodal zones is more likely to be taken depending on concrete cover.

Good number of experiments was implemented to evaluate the size effect of concrete deep beams, however most of them did not address the effect of bearing plates size and concrete cover that govern the width of diagonal concrete strut. The width of concrete strut plays an impact role on the shear strength of the deep elements. Theoretically, increasing the concrete depth with keeping the width of bearing plates constant leads to a decrease in shear capacity. Part of that reduction in shear capacity can be related to the non-geometrically simulation of the tested specimens because such increasing in the section depth makes the inclined concrete strut of the larger beams slenderer than those of the smaller ones. In another words, the cross-section area of the strut is constant compared with the length of the strut that increases owing to the increase in the section depth.

To confirm the effect of bearing plates and concrete cover on the geometry of the diagonal strut (according to the STM), two groups of samples have been examined analytically using STM of American [32], European [30] and Canadian [31] codes. Both groups (A and B) have the same values of concrete compressive strength, shear span to depth ratio, modulus of elasticity, and beam width, of 50 MPa, 1.5, 45 GPa, and 200 mm, respectively. The only difference between those two groups is the bearing plates and concrete cover as shown in Table 3. In group A, the bearing plates (loading and supporting) and concrete cover have been kept constant with 250 mm and 60 mm, respectively for all depths. However, in group B, the change in the section depth has been accompanied with the constant ratios of bearing plates/overall depth and concrete cover/overall depth of 0.15h and 0.08h, respectively.

Table 3. Details of assumed samples

Sample	h (mm)	Loading and supporting plate size (mm)		Bottom concrete cover	
		Group A	Group B	Group A	Group B
S1	500	250	0.15h	60	0.08h
S2	1000	250	0.15h	60	0.08h
S3	1500	250	0.15h	60	0.08h

The normalized total load ($P_u/f_c b_w h$) vs overall depth (h) has been used to study the size effect, where P_u is the total load. The results showed that changing the section depth with keeping the width of bearing plates and concrete cover constant (group A) leads to a clear size effect, as shown in Figure 7. This reduction in the normalized load with an increase in the section depth could be attributed to the slenderness ratio (L_{strut}/W_{strut}) which is the length of the concrete strut to the width of the concrete strut. When the section depth increases, the length of the concrete strut, L_{strut}, increases, however, the width of the strut is constant, resulting in higher L_{strut}/W_{strut} when the section depth increases as shown in Figure 8. Therefore, the normalized load of lager beams reduces compared with that of smaller beams which has a stockier strut.

On the other hand, it was found that keeping the ratio of bearing plates/overall depth and concrete cover/overall depth constant with changing the section depth (group B) results in eliminating size effect totally, as shown in Figure 9. To the author's knowledge, size effect has eliminated in samples of group B because length to the width of the concrete strut (L_{strut}/W_{strut}) for all samples have been kept constant as shown in Figure 10. Experimentally, it is believed that size effect can be mitigated if the bearing plats and concrete cover are proportionated with the section depth. It is worth mentioning that some researchers [7-9] have confirmed that size effect can be mitigated significantly by keeping the width of bearing plates to the section size constant. This confirms that the predicted strength according to the STM is partially a function of concrete strut and scaling both the concrete cover and the bearing plates geometrically results in geometrically scaled concrete strut, giving no size effect.

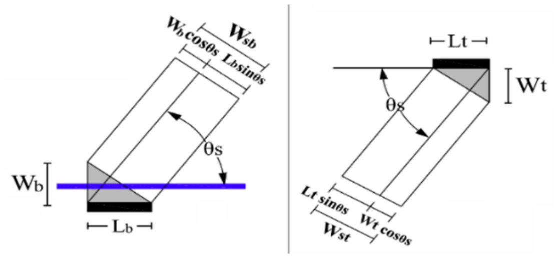

(a) (b)

Figure 6. Area of inclined strut (a) at the bottom (b) at the top

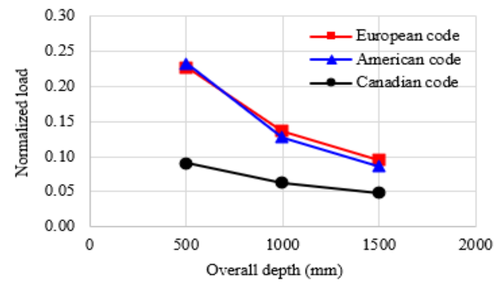

Figure 7. Size effect for samples of group A

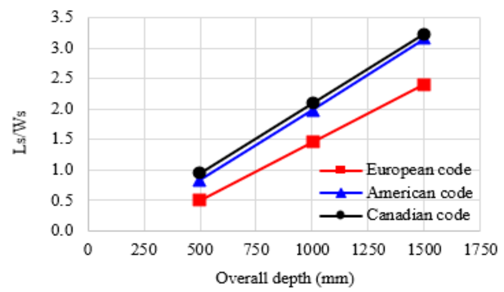

Figure 8. Relation between L_{strut}/W_{strut} and section depths of group A

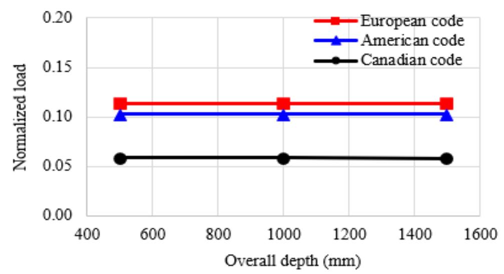

Figure 9. Size effect for samples of group B

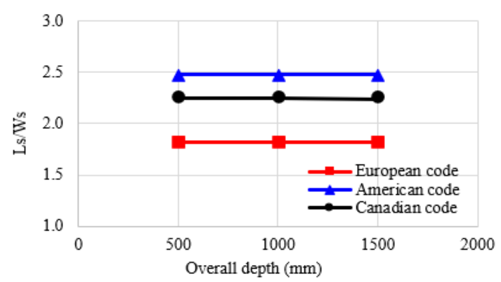

Figure 10. Relation between L_{strut}/W_{strut} and section depths of group B

5. COMPARISON WITH THE COLLECTED SPECIMENS

In order to assess the ability of the STM of American [32], European [30] and Canadian [31] codes to predict the load capacity of samples designed to investigate the size effect, a total of 25 simply supported beams reinforced with FRP bars have been gathered from the literature [4-7], as shown in Table 4. The collected specimens contain three types of FRP bars (GFRP, CFRP, and AFRP). The number of samples that is reinforced with GFRP, CFRP, and AFRP in the database is 16, 6, and 3, respectively. Compressive strengths of the collected beams are between 26 to 66 MPa, while shear span to depth ratios (a/d) and FRP longitudinal reinforcement ratios of collected beams range from 1 to 2 and 0.5 to 1.7, respectively. Eq. (1) is used to calculate the shear strength, while the effectiveness factor and stress limits in the nodal zones are taken according to the Tables 1 and 2, respectively. Since the width of a top horizontal compressive strut is unknown, iterative process has been used assuming that failure of horizontal concrete strut and inclined strut occurs at the same time. In such way, the minimum shear load causing strut failure can be calculated.

Table 4. Results of collected data

Authors	Sample	h (mm)	Normalized Pu $_{Exp.}$/ Normalized Pu $_{Calc.}$		
			ACI 318 (2014)	Euro code2 (2004)	CSA S806 (2012)
Andermatt and Lubell [7]	A1N	306	0.81	0.76	1.39
	B1N	608	0.64	0.60	1.10
	C1N	1003	0.62	0.61	1.12
	A2N	310	0.52	0.50	1.15
	B2N	606	0.52	0.49	1.10
	C2N	1005	0.47	0.46	1.04
	A3N	310	0.38	0.38	1.12
	B3N	607	0.34	0.36	1.03
	A4H	310	0.19	0.22	0.67
	B6H	610	0.18	0.21	0.64
Nehdi et al. [4]	CF-B-1	200	0.83	0.78	1.31
	CF-d-250	300	0.98	0.87	1.21
	CF-d-350	400	1.64	1.41	1.77
	F-B-1	200	0.59	0.56	1.36
	F-d-250	300	0.79	0.71	1.46
	F-d-350	400	1.16	1.05	1.99
Kim et al. [6]	A3D9S-1.7	240	0.82	0.75	2.01
	A4D9M-1.7	300	0.88	0.76	2.00
	A5D9L-1.7	360	0.96	0.81	2.05
	C3D9S-1.7	240	0.78	0.71	1.67
	C4D9M-1.7	300	0.70	0.60	1.38
	C5D9L-1.7	360	1.04	0.87	1.93
Abed et al. [5]	B1-FRP	300	0.39	0.39	0.83
	B6-FRP	350	0.39	0.37	0.68
	B7-FRP	400	0.52	0.48	0.79
Mean			0.69	0.62	1.31
CoV%			48	46	34

The results of the STM of American (ACI 318-14) and European (EN 1992-1-1) provisions are plotted in Figures 11 and 12, respectively. Table 4 presents the results of all collected data using the three codes. The results show that the mean of experimental-to-calculated normalized load values of those two provisions is 0.69 and 0.62 and coefficient of variation of 48% and 46%, respectively. Accordingly, it can be concluded that STM of American and European codes overestimates the load capacity. The overestimated results of the American and European codes for samples reinforced with FRP bars could be attributed to the fact that both codes neglect the modulus of elasticity and hence the longitudinal reinforcement bar type. This means that the predicted shear load will be the same for different bar types (FRP or steel) as long as the geometry of the deep beam and concrete compressive strength are kept constant.

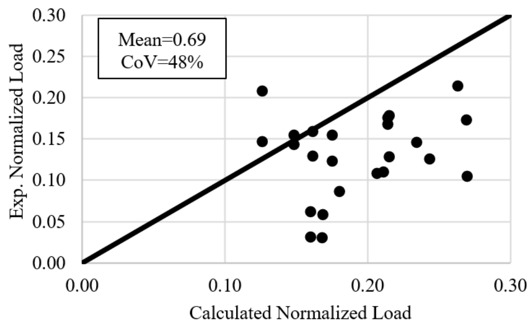

Figure 11. Experimental vs calculated normalized load according to the STM of the American code

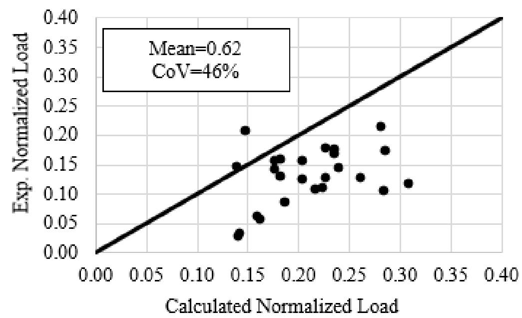

Figure 12. Experimental vs calculated normalized load according to the STM of the European code

The Canadian provision (CSA-S806-12) has underestimated the results with a mean and a coefficient of variation of experimental to predicted capacities of 1.31 and of 34%, respectively, as shown in Figure 13 and Table 4. Considering an inverse impact of strain on the effectiveness factor of the STM of the Canadian code, the low shear strength can be explained. The higher strain of FRP bars compared with that of steel bars results in a higher principal tensile strain (ε_1) that in return results in a lower effectiveness factor of concrete as shown in Table 2, and this will lead to a conservative shear and tie strength predictions for elements reinforced with FRP bars [35, 36]. However, it is expected that the Canadian standards are more suitable for the shear strength predications of steel bars reinforced deep elements than elements reinforced with FRP bars. Based on the aforementioned results, it can be concluded that the existing STMs of the American, European and Canadian codes are not recommended to evaluate the size effect of deep elements reinforced with FRP bars and, consequently, the STM model may need to be modified. However, STM of the Canadian code seems to be more acceptable with more ability to be developed. Besides, finite element is another technique can be addressed for buildings and large structural elements, such as deep beams, showing an economical approach to introduce a comprehensive analysis for such structures [37, 38].

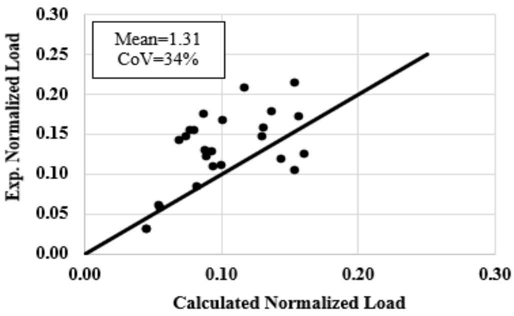

Figure 13. Experimental vs calculated normalized load according to the STM of the Canadian code

6. CONCLUSIONS

From the presented study, the following notes can be drawn:

1) Released energy can be considered as the main reason followed by aggregate interlock, while the out of plain action is active only in beams with large depths and have a high ratio of overall depth to beam width (*h/b*). Moreover, the brittle behaviour of the structural members makes size effect more pronounced.

2) From the STM point of view, no size effect is recorded as long as the bearing plates and concrete cover are proportionated with the section depth.

3) A considerable size effect was recorded when the bearing plates and concrete cover had not proportionated with the section depth.

4) An increase in the section depth with keeping the width of bearing plates and concrete cover constant leads to a higher slenderness ratio of the diagonal strut (L_{strut}/W_{strut}) and hence, a reduction in shear strength of the section.

5) The collected specimens showed that the STM of the American and European codes overestimated the shear capacity while the Canadian code gave a conservative prediction, highlighting the need of a suitable model for the shear strength predicting of deep beams reinforced with FRP bars.

REFERENCES

[1] Chen, H., Yi, W.J., Ma, Z.J., Hwang, H.J. (2020). Modeling of shear mechanisms and strength of concrete deep beams reinforced with FRP bars. Composite Structures, 234: 111715. https://doi.org/10.1016/j.compstruct.2019.111715

[2] Thomas, J., Ramadass, S. (2021). Prediction of the load and deflection response of concrete deep beams reinforced with FRP bars. Mechanics of Advanced Materials and Structures, 28(1): 43-66. https://doi.org/10.1080/15376494.2018.1549292

[3] Mohamed, A.M., Mahmoud, K., El-Salakawy, E.F. (2020). Behavior of simply supported and continuous concrete deep beams reinforced with GFRP bars. Journal of Composites for Construction, 24(4): 04020032. https://doi.org/10.1061/(ASCE)CC.1943-5614.0001039

[4] Nehdi, M., Omeman, Z., El-Chabib, H. (2008). Optimal efficiency factor in strut-and-tie model for FRP-reinforced concrete short beams with (1.5<a/d<2.5). Materials and Structures, 41(10): 1713-1727. https://doi.org/10.1617/s11527-008-9359-9

[5] Abed, F., El-Chabib, H., AlHamaydeh, M. (2012). Shear characteristics of GFRP-reinforced concrete deep beams without web reinforcement. Journal of Reinforced Plastics and Composites, 31(16): 1063-1073. https://doi.org/10.1177/0731684412450350

[6] Kim, D.J., Lee, J., Lee, Y.H. (2014). Effectiveness factor of strut-and-tie model for concrete deep beams reinforced with FRP rebars. Composites Part B: Engineering, 56: 117-125. https://doi.org/10.1016/j.compositesb.2013.08.009

[7] Andermatt, M.F., Lubell, A.S. (2013). Strength modeling of concrete deep beams reinforced with internal fiber-reinforced polymer. ACI Structural Journal, 110(4): 595. https://doi.org/10.14359/51685745

[8] Tan, K.H., Cheng, G.H., Zhang, N. (2008). Experiment to mitigate size effect on deep beams. Magazine of Concrete Research, 60(10): 709-723. https://doi.org/10.1680/macr.2007.00030

[9] Zhang, N., Tan, K.H. (2007). Size effect in RC deep beams: Experimental investigation and STM verification. Engineering Structures, 29(12): 3241-3254. https://doi.org/10.1016/j.engstruct.2007.10.005

[10] Yang, K.H., Ashour, A.F. (2007). Influence of section depth on the structural behaviour of reinforced concrete continuous deep beams. Magazine of Concrete Research, 59(8): 575-586. https://doi.org/10.1680/macr.2007.59.8.575

[11] Walravena, J., Lehwalter, N. (1994). Size effects in short beams loaded in shear. Structural Journal, 91(5): 585-593. https://doi.org/10.14359/4177

[12] Weibull, W. (1939). The phenomenon of rupture in solids. Royal Swedish Institute of Engineering Research (Ingenioersvetenskaps Akad. Handl.), Stockholm, 153: I-55. Google Scholar, 153.

[13] Tan, K.H., Lu, H.Y., Teng, S. (1999). Size effect in large prestressed concrete deep beams. Structural Journal, 96(6): 937-946. https://doi.org/10.14359/768

[14] Taylor, H.P. (1972). Shear strength of large beams. Journal of the Structural Division, 98(11): 2473-2490. https://doi.org/10.1061/JSDEAG.0003376

[15] Reinhardt, H.W. (1981). Similitude of brittle fracture of structural concrete. Advanced Mechanics of Reinforced Concrete, 175-184.

[16] Bazant, Z.P., Kim, J.K. (1984). Size effect in shear failure of longitudinally reinforced beams. American Concrete Institute., 81(5): 456-468. https://doi.org/10.14359/10696

[17] Bazant, Z.P., Kazemi, M.T. (1991). Size effect on diagonal shear failure of beams without stirrups. ACI Structural Journal, 88(3): 268-276. https://doi.org/10.14359/3097

[18] Tan, K.H., Lu, H.Y. (1999). Shear behavior of large reinforced concrete deep beams and code comparisons. Structural Journal, 96(5): 836-846. https://doi.org/10.14359/738

[19] Zinkaah, O.H., Ashour, A., Sheehan, T. (2019). Experimental tests of two-span continuous concrete deep beams reinforced with GFRP bars and strut-and-tie method evaluation. Composite Structures, 216: 112-126.

https://doi.org/10.1016/j.compstruct.2019.02.078
[20] Bazant, Z.P., Planas, J. (1997). Fracture and Size Effect in Concrete and Other Quasibrittle Materials. CRC Press.
[21] Wolinski, S., Hordijk, D.A., Reinhardt, H.W., Cornelissen, H.A. (1987). Influence of aggregate size on fracture mechanics parameters of concrete. International Journal of Cement Composites and Lightweight Concrete, 9(2): 95-103. https://doi.org/10.1016/0262-5075(87)90025-X
[22] CAN/CSA-S6-14. (2014). Canadian Highway Bridge Design Code.
[23] Kotsovos, M.D., Pavlovic, M.N. (1994). A possible explanation for size effects in structural concrete. Arch. Civil Eng., 40(2): 243-261.
[24] Zhang, N., Tan, K.H. (2007). Direct strut-and-tie model for single span and continuous deep beams. Engineering Structures, 29(11): 2987-3001. https://doi.org/10.1016/j.engstruct.2007.02.004
[25] Zinkaah, O.H., Ashour, A., Sheehan, T. (2019). 2D finite element analysis of GFRP reinforced concrete continuous deep beams with bond modelling. In Advanced Composites in Construction conference, ACIC2019 (Birmingham, UK, September 3: 5. https://doi.org/10.1016/j.engstruct.2007.02.004
[26] Zinkaah, O.H., Ashour, A. (2019). Load capacity predictions of continuous concrete deep beams reinforced with GFRP bars. In Structures, 19: 449-462. https://doi.org/10.1016/j.istruc.2019.02.007
[27] Schlaich, J., Schäfer, K., Jennewein, M. (1987). Toward a consistent design of structural concrete. PCI Journal, 32(3): 74-150. https://doi.org/10.15554/pcij.05011987.74.150
[28] Canadian Code (1984). Design of Concrete Structures for Buildings. A23.3, Canadian Standards Association, p. 281.
[29] ACI (American Concrete Institute) (2002). Building Code Requirements for Structural Concrete and Commentary, ACI, Farmington Hills, Michigan, p. 443.
[30] European Code. (2005). Eurocode 2: Design of Concrete Structures-Part 1-1: General Rules and Rules for Buildings. British Standard Institution, London.
[31] Canadian Code. (2012). Design and Construction of Building Components with Fiber-Reinforced Polymers. S806-2, Canadian Standards Association, p. 208.
[32] ACI (American Concrete Institute). (2014). Building Code Requirements for Structural Concrete and Commentary. ACI, Farmington Hills, Michigan, p. 619.
[33] Tan, K.H., Cheng, G.H. (2006). Size effect on shear strength of deep beams: Investigating with strut-and-tie model. Journal of Structural Engineering, 132(5): 673-685. https://doi.org/10.1061/(ASCE)07339445(2006)132:5(673)
[34] Tan, K., Cheng, G. Cheong, H. (2005). Size effect in shear strength of large beams behaviour and finite element modelling. Magazine of Concrete Research, 57(8): 497-509. https://doi.org/10.1680/macr.2005.57.8.497
[35] Zinkaah, O.H., Ashour, A., Sheehan, T. (2019). Size effect in GFRP reinforced continuous concrete deep beams. In Advanced Composites in Construction Conference, ACIC2019, Birmingham, UK.
[36] Zinkaah, O.H., Ashour, A., Sheehan, T. (2017). Assessment of strut and tie method for the prediction of shear strength of simply supported concrete deep beams reinforced with FRP bars. In Advanced Composites in Construction Conference (ACIC2017), Sheffield, UK.
[37] Fuyan, C. (2014). Study on the cracking pattern of concrete tower. Mathematical Modelling and Engineering Problem, 1(1): 5-10. https://doi.org/10.18280/mmep.010102
[38] Mohamed, K., Farghaly, A.S., Benmokrane, B., Neale, K. W. (2017). Nonlinear finite-element analysis for the behavior prediction and strut efficiency factor of GFRP-reinforced concrete deep beams. Engineering Structures, 137: 145-161. https://doi.org/10.1016/j.engstruct.2017.01.045